Continuum Mech. Thermodyn. (2018) 30:509–527
https://doi.org/10.1007/s00161-017-0618-2

ORIGINAL ARTICLE

Amir Reza Shahani · Hamid Sharifi Torki

Determination of the thermal stress wave propagation in orthotropic hollow cylinder based on classical theory of thermoelasticity

Received: 19 September 2017 / Accepted: 27 December 2017 / Published online: 15 January 2018

Abstract The thermoelasticity problem in a thick-walled orthotropic hollow cylinder is solved analytically using finite Hankel transform and Laplace transform. Time-dependent thermal and mechanical boundary conditions are applied on the inner and the outer surfaces of the cylinder. For solving the energy equation, the temperature itself is considered as boundary condition to be applied on both the inner and the outer surfaces of the orthotropic cylinder. Two different cases are assumed for solving the equation of motion: traction–traction problem (tractions are prescribed on both the inner and the outer surfaces) and traction–displacement (traction is prescribed on the inner surface and displacement is prescribed on the outer surface of the hollow orthotropic cylinder). Due to considering uncoupled theory, after obtaining temperature distribution, the dynamical structural problem is solved and closed-form relations are derived for radial displacement, radial and hoop stress. As a case study, exponentially decaying temperature with respect to time is prescribed on the inner surface of the cylinder and the temperature of the outer surface is considered to be zero. Owing to solving dynamical problem, the stress wave propagation and its reflections were observed after plotting the results in both cases.

Keywords Classical thermoelasticity · Orthotropic cylinder · Hankel transform · Stress wave

1 Introduction

Cylinders are one of the most applicable structures in the industrial areas. Meet the requirements of having materials which have diverse properties in different directions, has made a sharp rise in using orthotropic materials. Composite orthotropic thick-walled cylinders are capable of using in the various fields such as aerospace structures, space crafts, pressure vessels. Thermal loads are one of the most effectual loadings which numerous mechanical elements are affected by. In some cases, the intensity of these thermal loads in structures might lead to a substantial amount of thermal stresses which can be the main reason for making structural failure. Due to this widespread application, classical and generalized theories of thermoelasticity are developed. In the general form, the equations of thermoelasticity are coupled, i.e., a change in temperature field produces a strain and mutually time-dependent deformation leads to the change in temperature field. The traces of the coupling between temperature and displacement fields are seen in the classical thermoelasticity theory, where there are terms of the strain rate in the energy equation and terms of the temperature gradient in the equation of motion. The existence of these coupling terms between displacement and temperature fields makes the coupled classical theory of thermoelasticity very complicated. As a matter of fact, in many structures

Communicated by Andreas Öchsner.

A. R. Shahani (✉) · H. Sharifi Torki
K.N. Toosi University of Technology, P.O.B. 19991-43344, Tehran, Iran
E-mail: shahani@kntu.ac.ir

the coupling terms in the energy equation have a little impact on the temperature and stress field distribution. Due to the complexity in solving the coupled equations alongside the negligible effect of the coupling terms in reality, ignoring the coupling terms in the energy equations seems rational.

Yen and Krimser [1] presented a solution for determining thermal stresses in an isotropic cylinder which is subjected to axisymmetric thermal load. Both steady state and transient stresses are considered, and the solution is obtained by constructing the thermoelastic displacement potential and the bi-harmonic Love function.

Kardomateas [2] used a displacement approach to obtain the steady-state thermal stresses and displacements in an orthotropic elliptic cross-section cylinder. Temperature changes uniformly and the properties of the material are considered to be independent of the temperature.

Shahani and Nabavi [3] solved quasi-static thermoelasticity problem in a thick-walled hollow cylinder using finite Hankel transform. Time-dependent thermal boundary condition is applied on the inner surface and in case of mechanical boundary conditions traction–displacement and traction–traction problems are considered.

Analytical solution of quasi-static and dynamic uncoupled thermoelasticity problem in a thick-walled isotropic sphere presented by Shahani and Momeni [4] in 2014. The boundary conditions are considered to be time dependent and as a case study for dynamical problem, constant temperature is prescribed on the inner boundary, and both the inner and the outer boundaries are traction free. They [5] also solved the coupled thermoelasticity problem in a thick-walled isotropic sphere for the first time in 2013. Likewise the previous work, the problem is solved analytically and closed-form relations are extracted for the stress components.

Yee and Moon [6] presented a closed-form analytical solution for plane stress uncoupled quasi-static problem in an orthotropic hollow cylinder. Fourier–Bessel eigenfunction expansions are used for characterizing the temperature field distribution, and the corresponding thermal stresses are calculated using stress–stress function relations. The hollow orthotropic cylinder is subjected to an arbitrary temperature distribution, and thermal boundary conditions are considered to be homogenous.

Wang [7] studied the history and distribution of dynamic thermal stress in an isotropic cylinder. The cylinder is subjected to rapid arbitrary heating, and a uniform temperature is considered in the entire hollow cylinder which makes the problem uncoupled. The elastic displacement field is solved applying finite Hankel transform.

Chao et al. [8] presented an elastodynamic solution for the thermal dynamic stresses in an orthotropic thick cylindrical shell. The solution was obtained using finite Hankel transform and Laplace transform. The main disadvantage of this work is that the heat conduction equation is not solved as was the case in [7], and in an example, a constant temperature distribution is assumed for obtaining stress fields. Following the same approach, Ding et al. [9] solved dynamic plane strain thermoelasticity problem for a non-homogeneous orthotropic cylindrical shell using the orthogonal expansion technique.

Jabbari et al. [10] presented an analytical solution for coupled classical thermoelasticity in cylindrical coordinates, and the properties of material are considered to be isotropic. The Fourier expansion and eigenfunction method are used in solving partial differential equations.

Goshima and Miyao [11] analyzed transient thermal stresses in a long hollow isotropic circular cylinder. There is an internal heat generation due to γ-ray radiation, and both inner and outer surfaces of the cylinder are cooled by heat convection. The Laplace transform and Green's function are used for solving the problem. The inertia terms in the equations are neglected, and the properties of the material are independent of temperature.

Zhang et al. [12] derived an analytical solution for determining thermal stresses in a multilayered composite pressure vessel with closed ends subjected to thermal load and internal pressure. The problem is considered to be steady state, and the finite element method is used to validate the analytical results of this work.

Abd-allah et al. [13] studied the dynamic uncoupled thermal stresses in a long transversely isotropic solid circular cylinder. A constant temperature is applied to a specific portion of the surface, and the temperature of the other sections is considered to be zero. They used Fourier transform and theory of complex variables to obtain the solution of heat conduction equation, and Bessel functions series for longitudinal wave equation.

Kouchakzadeh and Entezari [14] solved the coupled thermoelasticity problem in an isotropic rotating disk analytically. The inner surface of the disk is subjected to a heat flux, and the outer surface temperature is considered to be zero. As well as this, the outer surface mechanical boundary condition is traction free and the inner one is assumed to be radially fixed.

Shahani and Sharifi [15] solved uncoupled dynamic thermoelasticity problem in an isotropic hollow cylinder. They solved the problem using the finite Hankel transform and Laplace transform. Time-dependent thermal and mechanical boundary conditions are prescribed on the inner and the outer surfaces.

Marin [16] studied the existence and the uniqueness of general solutions for the boundary value problems in elasticity of dipolar martials with voids. The theory of bodies with voids can be used in investigation the elastic

behavior of porous materials. The problem is considered to be elastostatic, and the material is anisotropic and non-homogenous.

Marin [17] obtained the harmonic vibrations in thermoelasticity of a cylinder which is made of microstretch anisotropic homogeneous material. One plane end of the cylinder is subjected to time varying harmonic boundary condition, and a thermal load is applied on the other end plane. He showed that the amplitude of the vibrations decays exponentially with the distance to the base.

Sharma and Marin [18] investigated wave propagation and reflection in micropolar thermoelastic solid in a half-plane using two-temperature theory of thermoelasticity. They obtained closed-form relations for amplitude ratios and showed that these ratios are functions of incidence angle, frequency and thermoelastic properties of the medium.

In this paper, uncoupled thermoelasticity problem in an orthotropic hollow cylinder is solved analytically. For the thermal boundary conditions, the inner and the outer surfaces of the cylinder are exposed to temperature which is known as the Dirichlet. Also for the mechanical boundary conditions, two different cases are considered: traction–traction problem (tractions are prescribed on both the inner and the outer surfaces) and traction–displacement (traction is prescribed on the inner surface and displacement is prescribed on the outer surface of the hollow orthotropic cylinder). The problem is solved using an innovative technique combined with the finite Hankel transform. The temperature field and the distribution of stress components are presented in closed-form relations. Distributions of the temperature field and the stress components for the two different mechanical boundary conditions are presented as figures. Due to considering inertia term in the equation of motion and solving the dynamical problem, the thermal stress wave and the reflection of stress wave into medium from the surfaces were observed after plotting the results. To validate the solution, the special case of a hollow cylinder subjected to the uniform constant temperature distribution is considered and the results are compared with those obtained by Ding et al. [9] which shows complete agreement. As well as this, comparing the results of this work with the results of the isotropic cylinder which was presented by Shahani and Sharifi [15], implies the accuracy and the precision of the solution.

2 Formulation

Consider a hollow orthotropic circular cylinder with inner and outer radii a and b, respectively. The cylinder is long enough in the axial direction to satisfy the plane strain condition. In addition the cylinder is subjected to symmetric boundary conditions. Due to symmetry, there is only radial dependence of the temperature and displacement distributions and stresses and strains become independent of the circumferential coordinate. Thus, the relations between stress and strain components are [19]:

$$\begin{bmatrix} \sigma_{rr} \\ \sigma_{\varphi\varphi} \\ \sigma_{zz} \\ \tau_{\varphi z} \\ \tau_{rz} \\ \tau_{r\varphi} \end{bmatrix} = \begin{bmatrix} c_{11} & c_{12} & c_{13} & 0 & 0 & 0 \\ c_{12} & c_{22} & c_{23} & 0 & 0 & 0 \\ c_{13} & c_{23} & c_{33} & 0 & 0 & 0 \\ 0 & 0 & 0 & c_{44} & 0 & 0 \\ 0 & 0 & 0 & 0 & c_{55} & 0 \\ 0 & 0 & 0 & 0 & 0 & c_{66} \end{bmatrix} \begin{bmatrix} \varepsilon_{rr} - \alpha_r \Delta T \\ \varepsilon_{\varphi\varphi} - \alpha_\varphi \Delta T \\ \varepsilon_{zz} - \alpha_z \Delta T \\ \gamma_{\varphi z} \\ \gamma_{rz} \\ \gamma_{r\varphi} \end{bmatrix} \tag{1}$$

where c_{ij} are the elastic constants and α_r, α_φ and α_z are thermal expansion coefficients in r, φ and z directions, respectively. The relations between c_{ij} and elastic moduli are [20]:

$$\begin{aligned} c_{11} &= \frac{(1-\nu_{23}\nu_{32})}{1-\nu_t} E_1; \qquad c_{12} = \frac{(\nu_{21}+\nu_{31}\nu_{23})}{1-\nu_t} E_1; \\ c_{22} &= \frac{(1-\nu_{13}\nu_{31})}{1-\nu_t} E_2; \qquad c_{13} = \frac{(\nu_{31}+\nu_{21}\nu_{32})}{1-\nu_t} E_1; \\ c_{33} &= \frac{(1-\nu_{12}\nu_{21})}{1-\nu_t} E_3; \qquad c_{23} = \frac{(\nu_{32}+\nu_{12}\nu_{31})}{1-\nu_t} E_2; \\ c_{44} &= G_{23}; \qquad c_{55} = G_{13}; \qquad c_{66} = G_{12}; \end{aligned} \tag{2}$$

where ν_{ij} are the Poisson's ratios and:

$$\nu_t = \nu_{12}\nu_{21} + \nu_{23}\nu_{32} + \nu_{13}\nu_{31} + \nu_{12}\nu_{23}\nu_{31} + \nu_{21}\nu_{32}\nu_{13} \tag{3}$$

where 1, 2 and 3 represent r, φ and z directions, respectively. Due to symmetry, one can conclude $\tau_{r\varphi} = \tau_{rz} = \tau_{z\varphi} = 0$, and so, the equations of motion reduce to:

$$\frac{\partial \sigma_{rr}}{\partial r} + \frac{1}{r}\left(\sigma_{rr} - \sigma_{\varphi\varphi}\right) = \rho\ddot{u} \tag{4}$$

in which ρ is the density. The strains components can be expressed in terms of the only non-vanishing displacement component, i.e., the radial displacement u as follows:

$$\varepsilon_{rr} = \frac{\partial u}{\partial r};\ \varepsilon_{\varphi\varphi} = \frac{u}{r};\ \varepsilon_{r\varphi} = \varepsilon_{\varphi z} = \varepsilon_{zr} = 0 \tag{5}$$

Substituting Eq. (5) into Eq. (1) and using Eq. (4) give the equation of motion in terms of displacement in the following form:

$$\frac{\partial^2 u}{\partial r^2} + \frac{1}{r}\frac{\partial u}{\partial r} - \frac{c_{22}}{c_{11}}\frac{u}{r^2} - \frac{\beta_{11}}{c_{11}}\frac{\partial \theta}{\partial r} + \frac{1}{r}\theta\left(\frac{\beta_{22} - \beta_{11}}{c_{11}}\right) = \frac{\rho}{c_{11}}\ddot{u} \tag{6}$$

where

$$\beta_{11} = c_{11}\alpha_r + c_{12}\alpha_\varphi + c_{13}\alpha_z \tag{7a}$$

$$\beta_{22} = c_{12}\alpha_r + c_{22}\alpha_\varphi + c_{23}\alpha_z \tag{7b}$$

and

$$\theta = T\left(r, t\right) - T_0 \tag{8}$$

where T_0 is the reference temperature at which the cylinder is stress free. The heat conduction equation in cylindrical coordinate system and for an orthotropic material takes the following form [21]:

$$k_1\frac{1}{r}\frac{\partial}{\partial r}\left(r\frac{\partial T}{\partial r}\right) + k_2\frac{1}{r^2}\frac{\partial^2 T}{\partial \varphi^2} + k_3\frac{\partial^2 T}{\partial z^2} + W = \rho c\frac{\partial T}{\partial t} \tag{9}$$

in which ρ is the density, c the specific heat, W the internal heat generation and k_1, k_2, k_3 are the thermal conductivity in r, φ, z directions, respectively. For the case of symmetric thermal boundary condition and in the absence of the internal heat generation, temperature distribution becomes independent of φ and z; thus, Eq. (9) is reduced to:

$$k_1\frac{1}{r}\frac{\partial}{\partial r}\left(r\frac{\partial T}{\partial r}\right) = \rho c\frac{\partial T}{\partial t} \tag{10}$$

Therefore, the equations of the uncoupled thermoelasticity problem in an orthotropic hollow cylinder are:

$$\frac{\partial^2 \theta}{\partial r^2} + \frac{1}{r}\frac{\partial \theta}{\partial r} = \frac{1}{\alpha^*}\frac{\partial \theta}{\partial t} \tag{11a}$$

$$\frac{\partial^2 u}{\partial r^2} + \frac{1}{r}\frac{\partial u}{\partial r} - \frac{\nu^2}{r^2}u - \frac{\beta_{11}}{c_{11}}\frac{\partial \theta}{\partial r} + \frac{1}{r}\theta\left(\frac{\beta_{22} - \beta_{11}}{c_{11}}\right) = \gamma^2\ddot{u} \tag{11b}$$

where

$$\alpha^* = \frac{k_1}{\rho c} \tag{12a}$$

$$\nu^2 = \frac{c_{22}}{c_{11}} \tag{12b}$$

$$\gamma^2 = \frac{\rho}{c_{11}} \tag{12c}$$

Two terms of the left-hand side of Eq. (11b) cause the interaction of thermal field on the mechanical field. The non-vanishing stress components are σ_{rr} and $\sigma_{\theta\theta}$ which are related to the displacement component and the temperature as follows:

$$\sigma_{rr} = c_{11}\frac{\partial u}{\partial r} + c_{12}\frac{u}{r} - \beta_{11}\theta \tag{13a}$$

$$\sigma_{\theta\theta} = c_{12}\frac{\partial u}{\partial r} + c_{22}\frac{u}{r} - \beta_{22}\theta \tag{13b}$$

3 Solution of the heat conduction equation

To solve the energy equation, the boundary and initial conditions are assumed in the following form:

$$\frac{\partial^2\theta}{\partial r^2}+\frac{1}{r}\frac{\partial\theta}{\partial r}-\frac{1}{\alpha^*}\frac{\partial\theta}{\partial t}=0 \tag{14a}$$

$$\theta\left(a,t\right)=f\left(t\right) \tag{14b}$$

$$\theta\left(b,t\right)=g\left(t\right) \tag{14c}$$

$$\theta\left(r,0\right)=0 \tag{14d}$$

The solutions of Eq. (14a) can be accomplished using the finite Hankel transform defined as [22]:

$$H\left[\theta\left(r,t\right);\zeta_n\right]=\bar{\theta}\left(\zeta_n,t\right)=\int_a^b r\theta\left(r,t\right)K_1\left(\zeta_n,r\right)\mathrm{d}r \tag{15}$$

where $K_1\left(\zeta_n,r\right)$ is the kernel of the transformation. Choosing the proper kernel depends on the form of the equation and the boundary conditions. The kernel of transformation for the present problem is as follows [23]:

$$K_1\left(r,\zeta_n\right)=\mathrm{J}_0\left(\zeta_n r\right)\mathrm{Y}_0\left(\zeta_n a\right)-\mathrm{J}_0\left(\zeta_n a\right)\mathrm{Y}_0\left(\zeta_n r\right) \tag{16}$$

where ζ_n's are the positive roots of the following characteristics equation:

$$\mathrm{J}_0\left(\zeta_n b\right)\mathrm{Y}_0\left(\zeta_n a\right)-\mathrm{J}_0\left(\zeta_n a\right)\mathrm{Y}_0\left(\zeta_n b\right)=0 \tag{17}$$

The inverse transform is defined as [23]:

$$H^{-1}\left[\bar{\theta}\left(\zeta_n,t\right);r\right]=\theta\left(r,t\right)=\sum_{n=1}^{\infty}a_n\bar{\theta}\left(\zeta_n,t\right)K_1\left(r,\zeta_n\right) \tag{18}$$

where

$$a_n=\frac{1}{\int_a^b r K_1^2\left(r,\zeta_n\right)\mathrm{d}r}=\frac{\pi^2}{2}\frac{\zeta_n^2\{\mathrm{J}_0\left(\zeta_n b\right)\}^2}{\{\mathrm{J}_0\left(\zeta_n a\right)\}^2-\{\mathrm{J}_0\left(\zeta_n b\right)\}^2} \tag{19}$$

Applying the finite Hankel transform to Eq. (14a) yields:

$$\frac{\partial\bar{\theta}}{\partial t}+\alpha^*\zeta_n^2\bar{\theta}\left(\zeta_n t\right)=\alpha^*\left[\frac{2\mathrm{J}_0\left(\zeta_n a\right)}{\pi\mathrm{J}_0\left(\zeta_n b\right)}g\left(t\right)-\frac{2}{\pi}f\left(t\right)\right]=A_1\left(t\right) \tag{20}$$

Eq. (20) is non-homogeneous ordinary differential equation, the solution of which can be easily obtained as follows:

$$\bar{\theta}\left(\zeta_n t\right)=\int_0^t A_1\left(\tau\right)\mathrm{e}^{-\alpha^*\zeta_n^2(t-\tau)}\mathrm{d}\tau \tag{21}$$

Using the inversion relations, Eq. (18a), we have:

$$\theta\left(r,t\right)=\sum_{n=1}^{\infty}a_n K_1\left(r,\zeta_n\right)\int_0^t A_1\left(\tau\right)\mathrm{e}^{-\alpha^*\zeta_n^2(t-\tau)}\mathrm{d}\tau \tag{22}$$

4 Solution of the equation of motion

For solving the equation of motion, two types of the boundary conditions are considered. In the first case, tractions are applied both on the inner and the outer surfaces of the orthotropic cylinder and in the second case the traction is applied on the inner surface and the displacement boundary condition on the outer one. To solve the displacement equation, $u\left(r,t\right)$ is resolved into two components:

$$u\left(r,t\right)=u_1\left(r,t\right)+u_2\left(r,t\right) \tag{23}$$

In the following, the solution for each of the introduced mechanical boundary conditions is presented.

4.1 Case 1: Traction–Traction

In this case, both the inner and the outer surfaces of the cylinder are subjected to the traction boundary conditions:

$$\sigma_{rr}(a,t) = P_1(t) \tag{24a}$$
$$\sigma_{rr}(b,t) = P_2(t) \tag{24b}$$

As is seen, the mechanical boundary conditions are considered to be time dependent and in a general form. By substituting (24a) and (24b) in (13a), we have:

$$\frac{\partial u}{\partial r}\Big|_{r=a} + h_1 u(a,t) = B_1(t) \tag{25a}$$
$$\frac{\partial u}{\partial r}\Big|_{r=b} + h_2 u(b,t) = B_2(t) \tag{25b}$$

where

$$h_1 = \frac{c_{12}}{c_{11}a} \tag{26a}$$
$$h_2 = \frac{c_{12}}{c_{11}b} \tag{26b}$$
$$B_1(t) = \frac{1}{c_{11}}P_1(t) + \frac{\beta_{11}}{c_{11}}f(t) \tag{26c}$$
$$B_2(t) = \frac{1}{c_{11}}P_2(t) + \frac{\beta_{11}}{c_{11}}g(t) \tag{26d}$$

The initial conditions for the displacement field are:

$$u(r,0) = F_2(r) \tag{27a}$$
$$\dot{u}(r,0) = F_3(r) \tag{27b}$$

where $F_2(r)$ and $F_3(r)$ are known functions of the radial position and a dot over the quantity is the partial derivative of it with respect to time. As is mentioned before, for solving displacement equation, it should be separated into two parts. The boundary conditions are allocated to the first homogenous part and the initial conditions for the second non-homogenous part of the differential equation:

$$\frac{\partial^2 u_1}{\partial r^2} + \frac{1}{r}\frac{\partial u_1}{\partial r} - \frac{\nu^2}{r^2}u_1 - \gamma^2 \ddot{u}_1 = 0 \tag{28a}$$
$$\frac{\partial u_1}{\partial r}\Big|_{r=a} + h_1 u_1(a,t) = B_1(t) \tag{28b}$$
$$\frac{\partial u_1}{\partial r}\Big|_{r=b} + h_2 u_1(b,t) = B_2(t) \tag{28c}$$
$$u_1(r,0) = 0 \tag{28d}$$
$$\dot{u}_1(r,0) = 0 \tag{28e}$$

and

$$\frac{\partial^2 u_2}{\partial r^2} + \frac{1}{r}\frac{\partial u_2}{\partial r} - \frac{\nu^2}{r^2}u_2 - \gamma^2 \ddot{u} = \frac{\beta_{11}}{c_{11}}\frac{\partial \theta}{\partial r} - \frac{1}{r}\theta\left(\frac{\beta_{22}-\beta_{11}}{c_{11}}\right) \tag{29a}$$
$$\frac{\partial u_2}{\partial r}\Big|_{r=a} + h_1 u_2(a,t) = 0 \tag{29b}$$
$$\frac{\partial u_2}{\partial r}\Big|_{r=b} + h_2 u_2(b,t) = 0 \tag{29c}$$
$$u_2(r,0) = F_2(r) \tag{29d}$$
$$\dot{u}_2(r,0) = F_3(r) \tag{29e}$$

The solutions of Eq. (28a) can be accomplished using the finite Hankel transform defined as [22]:

$$H\left[u_1\left(r,t\right);\xi_m\right]=\bar{u}_1\left(\xi_m,t\right)=\int_a^b ru_1\left(r,t\right)K_2\left(r,\xi_m\right)\mathrm{d}r \tag{30}$$

where $K_2\left(r,\xi_m\right)$ is the kernel of the transformation. Choosing the proper kernel depends on the form of the equation and the boundary conditions. The kernel of transformation for the present problem is as follows [23]:

$$K_2\left(r,\xi_m\right)=\left\{\mathrm{J}_\nu\left(\xi_m r\right)\left[\xi_m\mathrm{Y}'_\nu\left(\xi_m a\right)+h_1\mathrm{Y}_\nu\left(\xi_m a\right)\right]-\mathrm{Y}_\nu\left(\xi_m r\right)\left[\xi_m\mathrm{J}'_\nu\left(\xi_m a\right)+h_1\mathrm{J}_\nu\left(\xi_m a\right)\right]\right\} \tag{31}$$

where ξ_m's are the positive roots of the following characteristic equation:

$$\begin{aligned}&\left[\xi_m\mathrm{Y}'_\nu\left(\xi_m a\right)+h_1\mathrm{Y}_\nu\left(\xi_m a\right)\right]\left[\xi_m\mathrm{J}'_\nu\left(\xi_m b\right)+h_2\mathrm{J}_\nu\left(\xi_m b\right)\right]-\left[\xi_m\mathrm{Y}'_\nu\left(\xi_m b\right)+h_2\mathrm{Y}_\nu\left(\xi_m b\right)\right]\\&\times\left[\xi_m\,\mathrm{J}'_\nu\left(\xi_m a\right)+h_1\,\mathrm{J}_\nu\left(\xi_m a\right)\right]=0\end{aligned} \tag{32}$$

The inverse transform is defined as [23]:

$$H^{-1}\left[\bar{u}_1\left(\xi_m,t\right);r\right]=u_1\left(r,t\right)=\sum_{m=1}^{\infty}b_m\bar{u}_1\left(\xi_m,t\right)K_2\left(r,\xi_m\right) \tag{33}$$

where

$$b_m=\frac{1}{\int_a^b rK_2^2\left(r,\xi_m\right)\mathrm{d}r}=\frac{\pi^2\xi_m^2e_2^2}{2\left\{\left(h_2^2+\xi_m^2\left[1-\left(\frac{\nu}{\xi_m b}\right)^2\right]\right)e_1^2-\left(h_1^2+\xi_m^2\left[1-\left(\frac{\nu}{\xi_m a}\right)^2\right]\right)e_2^2\right\}} \tag{34}$$

in which

$$e_1=\xi_m\,\mathrm{J}'_\nu\left(\xi_m a\right)+h_1\mathrm{J}_\nu\left(\xi_m a\right) \tag{35a}$$

$$e_2=\xi_m\,\mathrm{J}'_\nu\left(\xi_m b\right)+h_2\mathrm{J}_\nu\left(\xi_m b\right) \tag{35b}$$

Applying the finite Hankel transform to Eq. (28a), yields:

$$\frac{\partial^2\bar{u}_1\left(\xi_m,t\right)}{\partial t^2}+\left(\frac{\xi_m}{\gamma}\right)^2\bar{u}_1\left(\xi_m,t\right)=\frac{1}{\gamma^2}\left[\frac{2e_1}{\pi e_2}B_2\left(t\right)-\frac{2}{\pi}B_1\left(t\right)\right]=A_2\left(t\right) \tag{36}$$

Eq. (36) is non-homogeneous ordinary differential equation, the solution of which can be easily obtained as follows:

$$\bar{u}_1\left(\xi_m,t\right)=\frac{\gamma}{\xi_m}\int_0^{\mathrm{t}}A_2\left(\tau\right)\sin\left(\frac{\xi_m}{\gamma}\left(\mathrm{t}-\tau\right)\right)\mathrm{d}\tau \tag{37}$$

Using the inversion relation, Eq. (33), we have:

$$u_1\left(r,t\right)=\sum_{m=1}^{\infty}\frac{\gamma}{\xi_m}b_mK_2\left(r,\xi_m\right)\int_0^t A_2\left(\tau\right)\sin\left(\frac{\xi_m}{\gamma}\left(t-\tau\right)\right)\mathrm{d}\tau \tag{38}$$

As is seen, the first equation has been solved. To solve the second part of the equations, $u_2\left(r,t\right)$ can be considered as the following form [5]:

$$u_2\left(r,t\right)=Y\left(t\right)K_2\left(r,\xi_m\right) \tag{39}$$

where $Y\left(t\right)$ is unknown function of time. It should be emphasized that the above form for $u_2\left(r,t\right)$ satisfies the related boundary conditions. Substituting Eq. (39) into (29a) yields to:

$$\left(\ddot{Y}+\left(\frac{\xi_m}{\gamma}\right)^2Y\right)K_2(r,\xi_m)=-\frac{a_n\bar{\theta}}{\gamma^2}\left[\frac{\beta_{11}}{c_{11}}\frac{\partial K_1\left(r,\zeta_n\right)}{\partial r}-\frac{1}{r}K_1\left(r,\zeta_n\right)\left(\frac{\beta_{22}-\beta_{11}}{c_{11}}\right)\right] \tag{40}$$

Using the orthogonality of the Bessel functions, the following equation can be obtained [22]:

$$\int_a^b r K_2(r,\xi_m)\, K_2\left(r,\xi_p\right) \mathrm{d}r = M_m \delta_{mp} \tag{41}$$

where δ is the Kronecker delta and:

$$M_m = \frac{1}{\xi_m^2}\left\{b^2 \frac{\mathrm{d}K_2}{\mathrm{d}r}\Big|_{r=b}^2 - a^2 \frac{\mathrm{d}K_2}{\mathrm{d}r}\Big|_{r=a}^2 + \left(\xi_m^2 - \nu^2\right)\left[b^2 K_2^2(b) - a^2 K_2^2(a)\right]\right\} \tag{42}$$

Multiplying Eq. (40) by $rK_2(r,\xi_m)$, integrating between a and b, and then using the orthogonality relation result in:

$$\ddot{Y} + \left(\frac{\xi_m}{\gamma}\right)^2 Y = \left\{-\frac{\int_a^b r K_2(r,\xi_m)\left[\frac{\beta_{11}}{c_{11}}\frac{\partial K_1(r,\zeta_n)}{\partial r} - \frac{1}{r}K_1(r,\zeta_n)\left(\frac{\beta_{22}-\beta_{11}}{c_{11}}\right)\right]\mathrm{d}r}{\gamma^2 M_m}\right\}\left(a_n\bar{\theta}\right) \tag{43}$$

To simplify the above equation, we introduce the following parameter:

$$U_1 = \left\{-\frac{\int_a^b r K_2(r,\xi_m)\left[\frac{\beta_{11}}{c_{11}}\frac{\partial K_1(r,\zeta_n)}{\partial r} - \frac{1}{r}K_1(r,\zeta_n)\left(\frac{\beta_{22}-\beta_{11}}{c_{11}}\right)\right]\mathrm{d}r}{\gamma^2 M_m}\right\} \tag{44}$$

Now, Eq. (43) can be written in the simplified form:

$$\ddot{Y} + \left(\frac{\xi_m}{\gamma}\right)^2 Y = U_1 a_n \bar{\theta} \tag{45}$$

The proper form of the initial conditions can be obtained by substituting Eq. (29d) into (39):

$$Y(0)\, K_2(r,\xi_m) = F_1(r) \tag{46}$$

Using the orthogonality relation, Eq. (41), yields to:

$$Y(0) = \frac{\int_a^b r K_2(r,\xi_m)\, F_1(r)\,\mathrm{d}r}{M_m} \tag{47}$$

The second initial condition can be obtained in a similar way:

$$\dot{Y}(0) = \frac{\int_a^b r K_2(r,\xi_m)\, F_2(r)\,\mathrm{d}r}{M_m} \tag{48}$$

Using Laplace transform and considering initial conditions lead to the following solution for the second part of the displacement equation.

$$Y(t) = \mathcal{L}^{-1}\left\{\frac{\mathcal{L}\left\{U_1\left[a_n\bar{\theta}\right]\right\} + sY(0) + \dot{Y}(0)}{\left[s^2 + \left(\frac{\xi_m}{\gamma}\right)^2\right]}\right\} \tag{49a}$$

$$\begin{aligned} Y(t) = {} & U_1 a_n \frac{\gamma}{\xi_m}\int_0^t \bar{\theta}(\zeta_n,\tau)\sin\left(\frac{\xi_m}{\gamma}(t-\tau)\right)\mathrm{d}\tau + \frac{\gamma}{\xi_m}\dot{Y}(0)\int_0^t \sin\left(\frac{\xi_m}{\gamma}(t-\tau)\right)\mathrm{d}\tau \\ & + Y(0)\int_0^t \cos\left(\frac{\xi_m}{\gamma}(t-\tau)\right)\mathrm{d}\tau \end{aligned} \tag{49b}$$

4.2 Case 2: Traction–Displacement

In the second case, the traction boundary condition is prescribed on the inner surface of the orthotropic cylinder and the displacement boundary condition on the outer one:

$$\sigma_{rr}(a,t) = P_1(t) \tag{50a}$$
$$u(b,t) = D_2(t) \tag{50b}$$

By substituting Eq. (50a) in (13a), we have:

$$\frac{\partial u}{\partial r}\Big|_{r=a} + h_1 u(a,t) = B_1(t) \tag{51a}$$
$$u(b,t) = B_2(t) \tag{51b}$$

where

$$h_1 = \frac{c_{12}}{c_{11}a} \tag{52a}$$
$$B_1(t) = \frac{1}{c_{11}} P_1(t) + \frac{\beta_{11}}{c_{11}} f(t) \tag{52b}$$
$$B_2(t) = D_2(t) \tag{52c}$$

The initial conditions for the displacement field are:

$$u(r,0) = F_2(r) \tag{53a}$$
$$\dot{u}(r,0) = F_3(r) \tag{53b}$$

where $F_2(r)$ and $F_3(r)$ are known functions of the radial position and a dot over the quantity is the partial derivative of it with respect to time. Likewise the first case, the following forms are considered for solving each part of the equation.

$$\frac{\partial^2 u_1}{\partial r^2} + \frac{1}{r}\frac{\partial u_1}{\partial r} - \frac{v^2}{r^2}u_1 - \gamma^2 \ddot{u}_1 = 0 \tag{54a}$$
$$\frac{\partial u_1}{\partial r}\Big|_{r=a} + h_1 u_1(a,t) = B_1(t) \tag{54b}$$
$$u_1(b,t) = B_2(t) \tag{54c}$$
$$u_1(r,0) = 0 \tag{54d}$$
$$\dot{u}_1(r,0) = 0 \tag{54e}$$

and

$$\frac{\partial^2 u_2}{\partial r^2} + \frac{1}{r}\frac{\partial u_2}{\partial r} - \frac{v^2}{r^2}u_2 - \gamma^2 \ddot{u}_2 = \frac{\beta_{11}}{c_{11}}\frac{\partial \theta}{\partial r} - \frac{1}{r}\theta\left(\frac{\beta_{22}-\beta_{11}}{c_{11}}\right) \tag{55a}$$
$$\frac{\partial u_2}{\partial r}\Big|_{r=a} + h_1 u_2(a,t) = 0 \tag{55b}$$
$$u_2(b,t) = 0 \tag{55c}$$
$$u_2(r,0) = F_2(r) \tag{55d}$$
$$\dot{u}_2(r,0) = F_3(r) \tag{55e}$$

The solutions of Eq. (54a) can be accomplished using the finite Hankel transform defined as [22]:

$$H\left[u_1(r,t);\lambda_q\right] = \bar{u}_1\left(\lambda_q,t\right) = \int_a^b r u_1(r,t) K_3\left(r,\lambda_q\right) \mathrm{d}r \tag{56}$$

where $K_3\left(r,\lambda_q\right)$ is the kernel of the transformation. The kernel of transformation for the present boundary condition is as follows [23]:

$$K_3\left(r,\lambda_q\right) = J_v\left(\lambda_q r\right) Y_v\left(\lambda_q b\right) - J_v\left(\lambda_q b\right) Y_v\left(\lambda_q r\right) \tag{57}$$

where λ_q's are the positive roots of the following characteristic equation:

$$Y_\nu\left(\lambda_q b\right)\left[\lambda_q J'_\nu\left(\lambda_q a\right)+h_1 J_\nu\left(\lambda_q a\right)\right]-J_\nu\left(\lambda_q b\right)\left[\lambda_q Y'_\nu\left(\lambda_q a\right)+h_1 Y_\nu\left(\lambda_q a\right)\right]=0 \tag{58}$$

The inverse transform is defined as [23]:

$$H^{-1}\left[\bar{u}_1\left(\lambda_q,t\right);r\right]=u_1\left(r,t\right)=\sum_{q=1}^{\infty}c_q\bar{u}_1\left(\lambda_q,t\right)K_3\left(r,\lambda_q\right) \tag{59}$$

where

$$c_q=\frac{1}{\int_a^b rK_3^2\left(r,\lambda_q\right)\mathrm{d}r}=\frac{\pi^2\lambda_q^2e_1^2}{2\{e_1^2-[J_\nu\left(\lambda_q b\right)]^2\left(h_1^2+\lambda_q^2\left[1-\left(\frac{\nu}{\lambda_q a}\right)^2\right]\right)\}} \tag{60}$$

in which

$$e_1=\lambda_q \mathrm{J}'_\nu\left(\lambda_q a\right)+h_1\mathrm{J}_\nu\left(\lambda_q a\right) \tag{61}$$

Applying the finite Hankel transform to Eq. (54a) yields:

$$\frac{\partial^2\bar{u}_1\left(\lambda_q,t\right)}{\partial t^2}+\left(\frac{\lambda_q}{\gamma}\right)^2\bar{u}_1\left(\lambda_q,t\right)=\frac{1}{\gamma^2}\left[-\frac{2J_\nu\left(\lambda_q b\right)}{\pi e_1}B_1\left(t\right)+\frac{2}{\pi}B_2\left(t\right)\right]=A_2\left(t\right) \tag{62}$$

The solution of the above differential equation can be obtained as follows:

$$\bar{u}_1\left(\lambda_q,t\right)=\frac{\gamma}{\lambda_q}\int_0^t A_2\left(\tau\right)\sin\left(\frac{\lambda_q}{\gamma}\left(t-\tau\right)\right)\mathrm{d}\tau \tag{63}$$

Using the inversion relation, Eq. (59), we have:

$$u_1\left(r,t\right)=\sum_{m=1}^{\infty}\frac{\gamma}{\lambda_q}c_qK_3\left(r,\lambda_q\right)\int_0^t A_2\left(\tau\right)\sin\left(\frac{\lambda_q}{\gamma}\left(t-\tau\right)\right)\mathrm{d}\tau \tag{64}$$

After obtaining the solution of the first part of the equation, to solve the second one, $u_2\left(r,t\right)$ can be considered as the following form [5]:

$$u_2\left(r,t\right)=Y\left(t\right)K_3\left(r,\lambda_q\right) \tag{65}$$

where $Y\left(t\right)$ is an unknown functions of time. Substituting Eq. (65) into (55a) yields to:

$$\left(\ddot{Y}+\left(\frac{\lambda_q}{\gamma}\right)^2Y\right)K_3\left(r,\lambda_q\right)=-\frac{a_n\bar{\theta}}{\gamma^2}\left[\frac{\beta_{11}}{c_{11}}\frac{\partial K_1\left(r,\zeta_n\right)}{\partial r}-\frac{1}{r}K_1\left(r,\zeta_n\right)\left(\frac{\beta_{22}-\beta_{11}}{c_{11}}\right)\right] \tag{66}$$

Using the orthogonality of the Bessel functions, the following equation can be obtained [22]:

$$\int_a^b rK_3\left(r,\lambda_q\right)K_3\left(r,\lambda_p\right)\mathrm{d}r=M_m\delta_{qp} \tag{67}$$

where δ is the Kronecker delta. Multiplying Eq. (66) by $rK_3\left(r,\lambda_q\right)$, integrating between a and b, and then using the orthogonality relations results in:

$$\ddot{Y}+\left(\frac{\lambda_q}{\gamma}\right)^2Y=\left\{-\frac{\int_a^b rK_3\left(r,\lambda_q\right)\left[\frac{\beta_{11}}{c_{11}}\frac{\partial K_1\left(r,\zeta_n\right)}{\partial r}-\frac{1}{r}K_1\left(r,\zeta_n\right)\left(\frac{\beta_{22}-\beta_{11}}{c_{11}}\right)\right]\mathrm{d}r}{\gamma^2M_m}\right\}\left(a_n\bar{\theta}\right) \tag{68}$$

Now, Eq. (68) can be simplified in the following form:

$$\ddot{Y}+\left(\frac{\lambda_q}{\gamma}\right)^2Y=U_2a_n\bar{\theta} \tag{69}$$

where

$$U_2 = \left\{ -\frac{\int_a^b r K_3\left(r, \lambda_q\right)\left[\frac{\beta_{11}}{c_{11}} \frac{\partial K_1(r,\zeta_n)}{\partial r} - \frac{1}{r} K_1\left(r, \zeta_n\right)\left(\frac{\beta_{22}-\beta_{11}}{c_{11}}\right)\right] \mathrm{d}r}{\gamma^2 M_m} \right\} \tag{70}$$

In a similar way, to obtain the proper initial conditions we have:

$$Y\left(0\right) = \frac{\int_a^b r K_3\left(r, \lambda_q\right) F_1\left(r\right) \mathrm{d}r}{M_m} \tag{71a}$$

$$\dot{Y}\left(0\right) = \frac{\int_a^b r K_3\left(r, \lambda_q\right) F_2\left(r\right) \mathrm{d}r}{M_m} \tag{71b}$$

Using Laplace transform and Eqs. (71a) and (71b), the solution of Eq. (69) can be obtained:

$$Y\left(t\right) = \mathcal{L}^{-1}\left\{ \frac{\mathcal{L}\left\{U_2\left[a_n \bar{\theta}\right]\right\} + sY\left(0\right) + \dot{Y}\left(0\right)}{\left[s^2 + \left(\frac{\lambda_q}{\gamma}\right)^2\right]} \right\} \tag{72a}$$

$$\begin{aligned} Y\left(t\right) = U_2 a_n \frac{\gamma}{\lambda_q} \int_0^t \bar{\theta}\left(\zeta_n, \tau\right) \sin\left(\frac{\lambda_q}{\gamma}\left(t-\tau\right)\right) \mathrm{d}\tau + \frac{\gamma}{\lambda_q} \dot{Y}\left(0\right) \int_0^t \sin\left(\frac{\lambda_q}{\gamma}\left(t-\tau\right)\right) \mathrm{d}\tau \\ + Y\left(0\right) \int_0^t \cos\left(\frac{\lambda_q}{\gamma}\left(t-\tau\right)\right) \mathrm{d}\tau \end{aligned} \tag{72b}$$

5 Numerical examples

In order to study the response of the orthotropic cylinder under external loads, two numerical examples are considered. The following material specifications are employed in the calculations [24]:

$$\begin{aligned} a = 1\,\mathrm{m};\ b = 2\,\mathrm{m};\ P_1 = P_2 = 0;\ \theta_0 = 100;\ \omega = 0.001;\ \alpha^* = .112E-6\,\mathrm{m}^2/\mathrm{s} \\ E_{11} = 19.8\,\mathrm{GPa};\ E_{22} = 48.3\,\mathrm{GPa};\ E_{33} = 19.8\,\mathrm{GPa};\ G_{12} = 8.9\,\mathrm{GPa}; \\ G_{23} = 8.9\,\mathrm{GPa};\ G_{31} = 6.19\,\mathrm{GPa};\ \nu_{12} = .27;\ \nu_{23} = .27;\ \nu_{31} = .3 \\ \alpha_{11} = 15E-6\,1/\mathrm{K};\ \alpha_{22} = 0.23E-6\,1/\mathrm{K};\ \alpha_{33} = 15E-6\,1/\mathrm{K}; \end{aligned}$$

In order to plot the distribution of temperature, it is considered that an exponentially decaying temperature is applied on the inner surface of the cylinder. So, the thermal boundary conditions and the initial condition are:

$$\theta\left(a, t\right) = \theta_0 \mathrm{e}^{-\omega t} \tag{73a}$$

$$\theta\left(b, t\right) = 0 \tag{73b}$$

$$\theta\left(r, 0\right) = 0 \tag{73c}$$

Considering the above equations and Eq. (20) yields:

$$A_1\left(t\right) = -\frac{2\alpha^* \theta_0 \mathrm{e}^{-\omega t}}{\pi} \tag{74}$$

Using Eqs. (74) and (21) leads to:

$$\bar{\theta}\left(\zeta_n t\right) = -\frac{2\alpha^* \theta_0}{\pi\left(\alpha^* \zeta_n^2 - \omega\right)}\left(\mathrm{e}^{-\omega t} - \mathrm{e}^{-\alpha^* \zeta_n^2 t}\right) \tag{75}$$

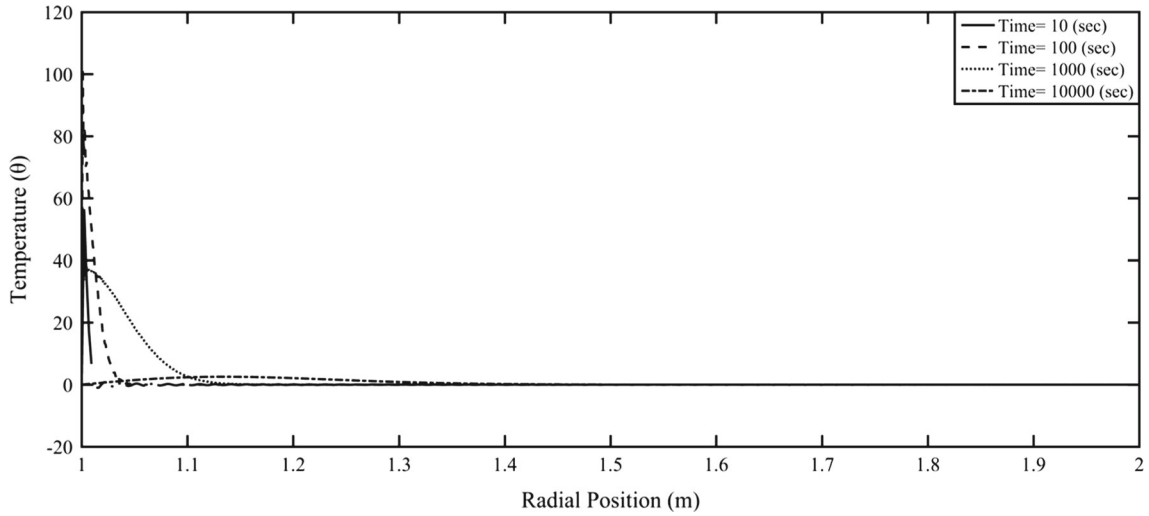

Fig. 1 Temperature distribution versus the radial distance

Substituting Eq. (75) into Eq. (22) results in:

$$\theta\left(r,t\right)=-\alpha^{*}\pi\theta_{0}\sum_{n=1}^{\infty}\frac{\zeta_{n}^{2}\{\mathrm{J}_{0}\left(\zeta_{n}b\right)\}^{2}}{\{\mathrm{J}_{0}\left(\zeta_{n}a\right)\}^{2}-\{\mathrm{J}_{0}\left(\zeta_{n}b\right)\}^{2}}\frac{\left(\mathrm{e}^{-\omega t}-\mathrm{e}^{-\alpha^{*}\zeta_{n}^{2}t}\right)}{\left(\alpha^{*}\zeta_{n}^{2}-\omega\right)}K_{1}\left(r,\zeta_{n}\right)\tag{76}$$

Figure 1 shows the distribution of the temperature through the thickness of the orthotropic cylinder. It can be seen that over time passing the temperature of each point increases so long as it reaches the steady-state condition which is zero temperature.

Due to the low thermal conductivity, it takes a lot of time to reach the steady-state condition.

The histories of the thermal stresses which are caused by this temperature distribution are presented in the following for each of the mechanical boundary conditions.

5.1 Case 1: Traction–Traction

As mentioned, in this case the tractions are prescribed on both the inner surface and the outer surface of the cylinder. Using the presented specifications leads to:

$$\sigma_{rr}\left(a,t\right)=0\tag{77a}$$

$$\sigma_{rr}\left(b,t\right)=0\tag{77b}$$

Considering Eqs. (26c), (26d) and (36), we have:

$$B_{1}=\frac{\beta_{11}}{c_{11}}\theta_{0}\mathrm{e}^{-\omega t}\tag{78a}$$

$$B_{2}=0\tag{78b}$$

$$A_{2}\left(t\right)=-\frac{2\theta_{0}\beta_{11}\mathrm{e}^{-\omega t}}{\pi\gamma^{2}c_{11}}\tag{78c}$$

Substituting the above equations in Eq. (37) yields to:

$$\bar{u}_{1}\left(\xi_{m}t\right)=\frac{2\theta_{0}\beta_{11}}{\pi c_{11}\left(\xi_{m}^{2}+\omega^{2}\gamma^{2}\right)}\left\{\frac{1}{\xi_{m}}\left[\xi_{m}\cos\left(\frac{\xi_{m}}{\gamma}t\right)-\gamma\omega\sin\left(\frac{\xi_{m}}{\gamma}t\right)\right]-\mathrm{e}^{-\omega t}\right\}\tag{79}$$

Thus, the final solution of the first part of the displacement component can be obtained in the following form:

$$u_{1}\left(r,t\right)=\frac{2\theta_{0}\beta_{11}}{\pi c_{11}}\sum_{m=1}^{\infty}\frac{b_{m}}{\left(\xi_{m}^{2}+\omega^{2}\gamma^{2}\right)}\left\{\cos\left(\frac{\xi_{m}}{\gamma}t\right)-\frac{\gamma\omega}{\xi_{m}}\sin\left(\frac{\xi_{m}}{\gamma}t\right)-\mathrm{e}^{-\omega t}\right\}K_{2}\left(r,\xi_{m}\right)\tag{80}$$

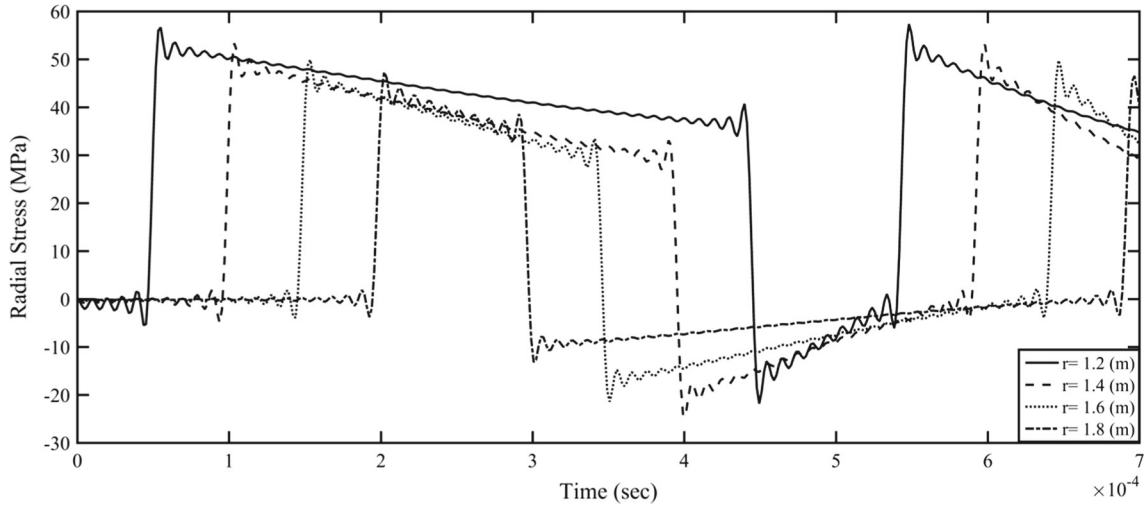

Fig. 2 History of dynamic radial stress for different radial positions (case i)

The section of the second part of the answer which was a function of time is obtained in the following form:

$$
\begin{aligned}
Y(t) = -\frac{2a_n\theta_0 U_1 \alpha^* \gamma}{\pi\left(\alpha^*\zeta_n^2 - \omega\right)\xi_m} \Bigg\{ & \frac{\left(\frac{\xi_m}{\gamma}\right) e^{-\omega t}}{\omega^2 + \left(\frac{\xi_m}{\gamma}\right)^2} \\
& - \frac{\left(\frac{\xi_m}{\gamma}\right)}{\omega^2 + \left(\frac{\xi_m}{\gamma}\right)^2} \cos\left(\frac{\xi_m}{\gamma} t\right) + \frac{\omega}{\omega^2 + \left(\frac{\xi_m}{\gamma}\right)^2} \sin\left(\frac{\xi_m}{\gamma} t\right) \\
& - \frac{\left(\frac{\xi_m}{\gamma}\right) e^{-\alpha^*\zeta_n^2 t}}{\left(\alpha^*\zeta_n^2\right)^2 + \left(\frac{\xi_m}{\gamma}\right)^2} + \frac{\left(\frac{\xi_m}{\gamma}\right)}{\left(\alpha^*\zeta_n^2\right)^2 + \left(\frac{\xi_m}{\gamma}\right)^2} \cos\left(\frac{\xi_m}{\gamma} t\right) \\
& - \frac{\alpha^*\zeta_n^2}{\left(\alpha^*\zeta_n^2\right)^2 + \left(\frac{\xi_m}{\gamma}\right)^2} \sin\left(\frac{\xi_m}{\gamma} t\right) \Bigg\}
\end{aligned}
\tag{81}
$$

Now, after determining the both parts of radial displacement component, the stress components distributions can be easily derived from Eqs. (13a) and (13b).

Figure 2 illustrates the dynamic radial stress history for the first case of the boundary conditions. As is seen, dilatation stress wave which is created by thermal boundary condition at the inner surface moves forward from the inner surface through the thickness of orthotropic cylinder. After colliding with the outer surface, the stress wave reflects into the medium but as reversed. The reason of this fact is considering traction free boundary condition for the outer surface of the orthotropic cylinder.

In point of fact, propagating tensile radial stress wave leads to producing compressive hoop stress. However, as is seen from Fig. 3, hoop stress component is tensile at the initial moments and it diminishes and turns into compressive passing time. This occurs due to the resistance of the nearby points in the medium which exerts to any point. But this resistance vanishes after the stress wave reaches to the nearby point.

5.2 Case 2: Traction–Displacement

The traction on the inner surface and the displacement on the outer surface are assumed as boundary conditions in this case. These types of boundary conditions can be stated as follows:

$$\sigma_{rr}(a, t) = 0 \tag{82a}$$

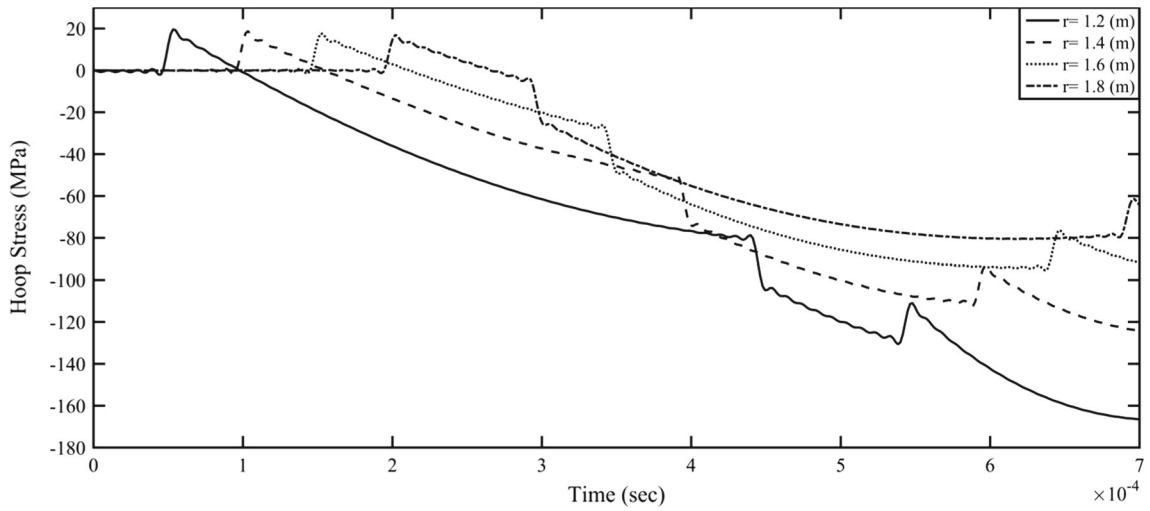

Fig. 3 History of dynamic hoop stress for different radial positions (case i)

$$u\left(b,t\right)=0 \tag{82b}$$

Considering Eqs. (52c), (52d) and (62), leads to:

$$B_1=\frac{\beta_{11}}{c_{11}}\theta_0 \mathrm{e}^{-\omega t} \tag{83a}$$

$$B_2=0 \tag{83b}$$

$$A_2\left(t\right)=-\frac{2\beta_{11}\theta_0 \mathrm{e}^{-\omega t}}{c_{11}\gamma^2\pi}\frac{J_\nu\left(\lambda_q b\right)}{e_1} \tag{83c}$$

Substituting Eq. (83c) into Eq. (63) yields:

$$\bar{u}_1\left(\lambda_q t\right)=\frac{2\theta_0\beta_{11}J_\nu\left(\lambda_q b\right)}{\pi c_{11}\left(\lambda_q^2+\omega^2\gamma^2\right)e_1}\left\{\frac{1}{\lambda_q}\left[\lambda_q\cos\left(\frac{\lambda_q}{\gamma}t\right)-\gamma\omega\sin\left(\frac{\lambda_q}{\gamma}t\right)\right]-\mathrm{e}^{-\omega t}\right\} \tag{84}$$

Therefore, the first part of the solution for displacement field can be obtained using Eq. (64):

$$u_1\left(r,t\right)=\frac{2\theta_0\beta_{11}}{\pi c_{11}}\sum_{m=1}^{\infty}\frac{c_q J_\nu\left(\lambda_q b\right)}{\left(\lambda_q^2+\omega^2\gamma^2\right)e_1}\left\{\left[\cos\left(\frac{\lambda_q}{\gamma}t\right)-\frac{\gamma\omega}{\lambda_q}\sin\left(\frac{\lambda_q}{\gamma}t\right)\right]-\mathrm{e}^{-\omega t}\right\}K_3\left(r,\lambda_q\right) \tag{85}$$

In addition, for the second part of solution we have:

$$Y\left(t\right)=-\frac{2a_n\theta_0U_2\alpha^*\gamma}{\pi\left(\alpha^*\zeta_n^2-\omega\right)\lambda_q}\left\{\frac{\left(\frac{\lambda_q}{\gamma}\right)\mathrm{e}^{-\omega t}}{\omega^2+\left(\frac{\lambda_q}{\gamma}\right)^2}\right.$$
$$\left.-\frac{\left(\frac{\lambda_q}{\gamma}\right)}{\omega^2+\left(\frac{\lambda_q}{\gamma}\right)^2}\cos\left(\frac{\lambda_q}{\gamma}t\right)+\frac{\omega}{\omega^2+\left(\frac{\lambda_q}{\gamma}\right)^2}\sin\left(\frac{\lambda_q}{\gamma}t\right)\right.$$

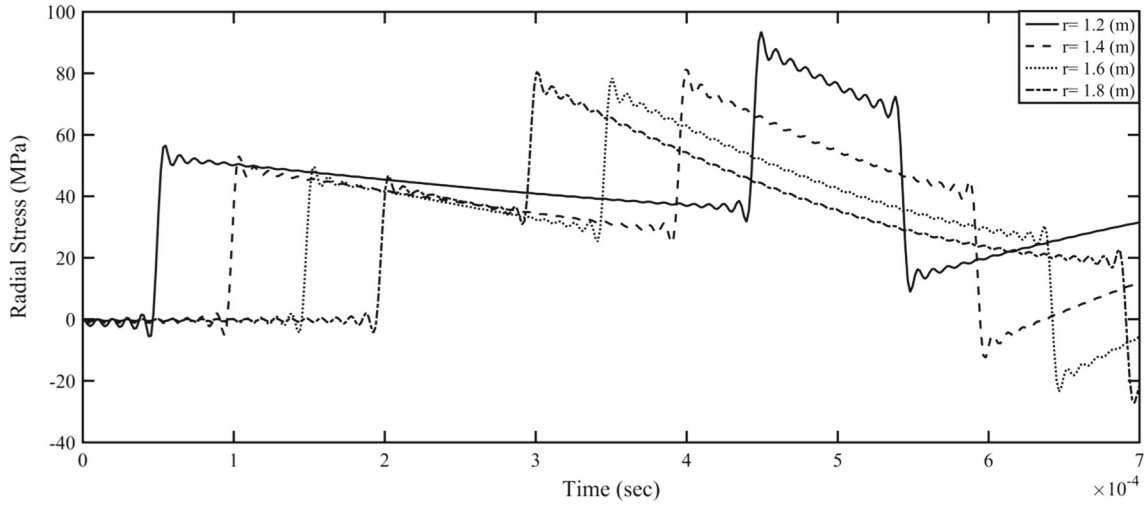

Fig. 4 History of dynamic radial stress for different radial positions (case ii)

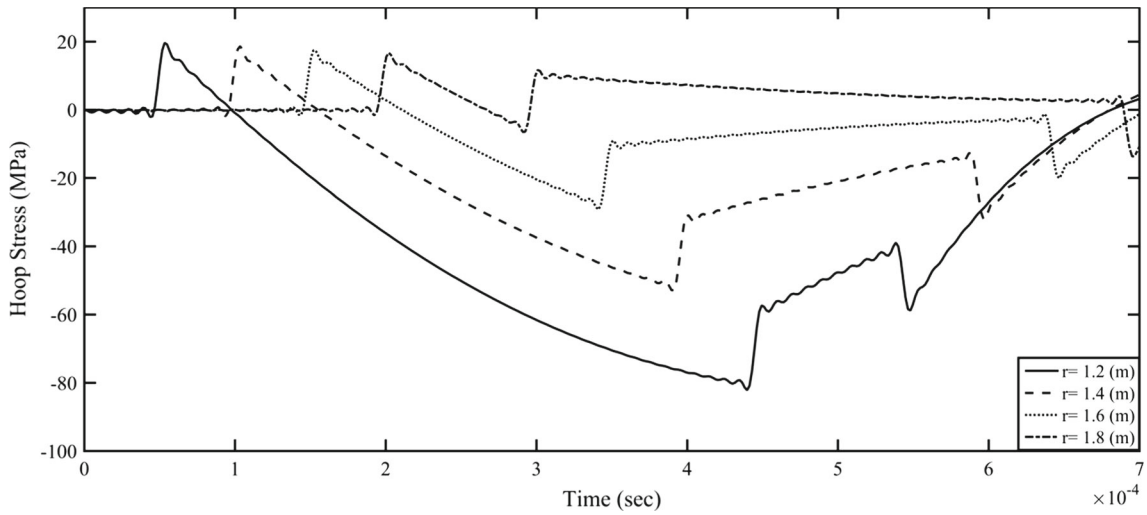

Fig. 5 History of dynamic hoop stress for different radial positions (case ii)

$$\left.-\frac{\left(\frac{\lambda_q}{\gamma}\right)e^{-\alpha^*\zeta_n^2 t}}{\left(\alpha^*\zeta_n^2\right)^2+\left(\frac{\lambda_q}{\gamma}\right)^2}+\frac{\left(\frac{\lambda_q}{\gamma}\right)}{\left(\alpha^*\zeta_n^2\right)^2+\left(\frac{\lambda_q}{\gamma}\right)^2}\cos\left(\frac{\lambda_q}{\gamma}t\right)\right.$$
$$\left.-\frac{\alpha^*\zeta_n^2}{\left(\alpha^*\zeta_n^2\right)^2+\left(\frac{\lambda_q}{\gamma}\right)^2}\sin\left(\frac{\lambda_q}{\gamma}t\right)\right\} \tag{86}$$

Using Eqs. (13a) and (13b), the radial and the hoop stress components can be obtained.

Figure 4 shows the dynamic radial stress history for the second case of the boundary conditions. As is seen, likewise the previous case, initiated dilatation stress wave at the inner surface moves forward from the inner surface of the orthotropic cylinder to the outer one. In spite of the traction–traction boundary condition, the stress wave which is reflected into the medium does not become reversed in this case. Considering the outer surface of the cylinder to be fixed causes the reality of reflecting the stress wave from the outer surface into medium as the same sign.

As is mentioned, tensile radial stress wave produces compressive hoop stress. It can be seen in Fig. 5, when the tensile radial stress wave reaches any radial position for the first time, the hoop stress component becomes

Table 1 Comparison between the instants of reaching dilatation wave to specific radial positions considered in Figs. 2 and 3 and Eq. (88)

Radial position (m)	Calculated using Eq. (88) (s)	Obtained using Fig. 2 (s)
$r = 1.2$	4.94×10^{-5}	4.915×10^{-5}
$r = 1.4$	9.88×10^{-5}	9.885×10^{-5}
$r = 1.6$	14.82×10^{-5}	14.85×10^{-5}
$r = 1.8$	19.76×10^{-5}	19.75×10^{-5}

tensile at the early moments due to the resistance of nearby points and after that it decreases gradually with time.

Dilatation wave velocity can be obtained using the following equation:

$$V_e = \frac{1}{\gamma} = \sqrt{\frac{c_{11}}{\rho}} = 4.049 \times 10^3 \,(\mathrm{m/s}) \tag{87}$$

Using the above equation, one can compute the first time when dilatation wave reaches any radial position. This value can be calculated using the following equation:

$$t^* = \frac{r - a}{V_e} \tag{88}$$

Table 1 indicates the values which are calculated with Eq. (88) and those which are obtained from Fig. 2.

6 Validation

6.1 Uniformly heated orthotropic cylinder

The present work is validated in a special case with the problem of orthotropic cylinder subjected to uniform temperature throughout the cylinder. In the mentioned problem, the energy equation has not been solved and a constant temperature is assumed for all radial sections of the cylinder and therefore there is no temperature gradient. The history of non-dimensional stress components is plotted in Figs. 6 and 7. Due to applying thermo-mechanical boundary conditions in the inner and the outer surfaces, there are two thermoelastic waves. The one moves outward from the inner surface, and the other propagates inward the medium from the outer surface. The corresponding results of Ding et al. [9] have been shown on the same figures. It is observed that the results of this work are in good agreement with the results of Ding et al. [9]. The following properties are employed in calculations:

$$\begin{aligned} a = 50\ \mathrm{mm};\ b = 100\ \mathrm{mm};\ \theta_0 = 200, \quad c_{11} = 17.075\ \mathrm{GPa} \\ c_{12} = 6.757\ \mathrm{GPa};\ c_{13} = 7.289\ \mathrm{GPa};\ c_{22} = 59.645\ \mathrm{GPa}; \\ c_{23} = 6.752\ \mathrm{GPa};\ c_{33} = 17.074\ \mathrm{GPa};\ \rho = 1700\ \mathrm{kg/m^3} \\ \alpha_{11} = 4E-5\,1/\mathrm{K};\ \alpha_{22} = 1E-5\,1/\mathrm{K};\ \alpha_{33} = 4E-5\,1/\mathrm{K}; \end{aligned}$$

The non-dimensional time relation used in the figures are defined as follows:

$$\bar{t} = \frac{V_e t}{a} \tag{89}$$

6.2 Pure thermal load in isotropic cylinder

As it is mentioned orthotropic cylinder has different mechanical and thermal properties in three different directions. By choosing the same amount for these properties in all directions, the orthotropic cylinder reduces to isotropic one. Indeed isotropic cylinder is a special case of orthotropic cylinder which has the same properties in different directions. The analytical solution of the thermoelasticity problem in isotropic cylinder which is

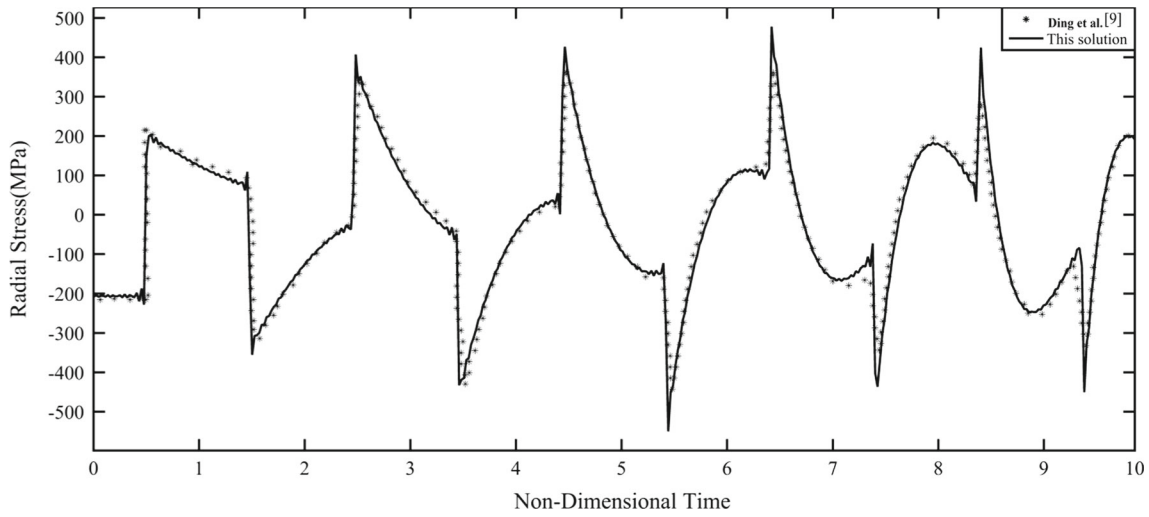

Fig. 6 Variation of radial stress for $r = (a + b)/2$

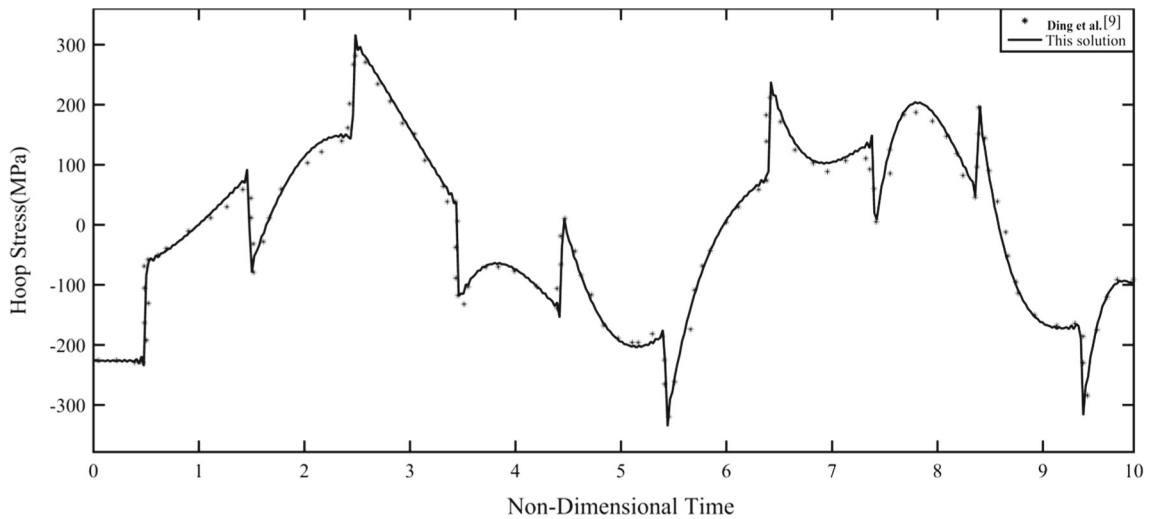

Fig. 7 Variation of hoop stress for $r = (a + b)/2$

subjected to transient thermal loading is also solved by Shahani and Sharifi [15]. The following properties are employed for comparing the result of the present work with those which are presented in [15].

$$a = 1\ \text{m};\quad b = 2\ \text{m};\ \nu = .3;\quad \theta_0 = 100\ \text{e}^{-\omega t};\ \omega = 0.001$$
$$E = 70\ \text{GPa};\quad \rho = 2707\ {}^{\text{kg}}/_{\text{m}^3};\ k = 204\ \text{w/mk}$$
$$\alpha = 23E - 6\,{}^{1}/_{\text{K}};\quad c = 903\ {}^{\text{J}}/_{\text{kg K}};\ T_0 = 293\ \text{K}$$

A time-decaying temperature is applied on the inner surface of the cylinder, and the outer surface temperature is considered to be zero. Figure 8 shows the history of temperature in isotropic cylinder.

Figures 9 and 10 indicate the history of radial and hoop stress. As is seen, considering the same properties in different directions in orthotropic cylinder leads to the same results as in isotropic cylinder which were presented by Shahani and Sharifi [15].

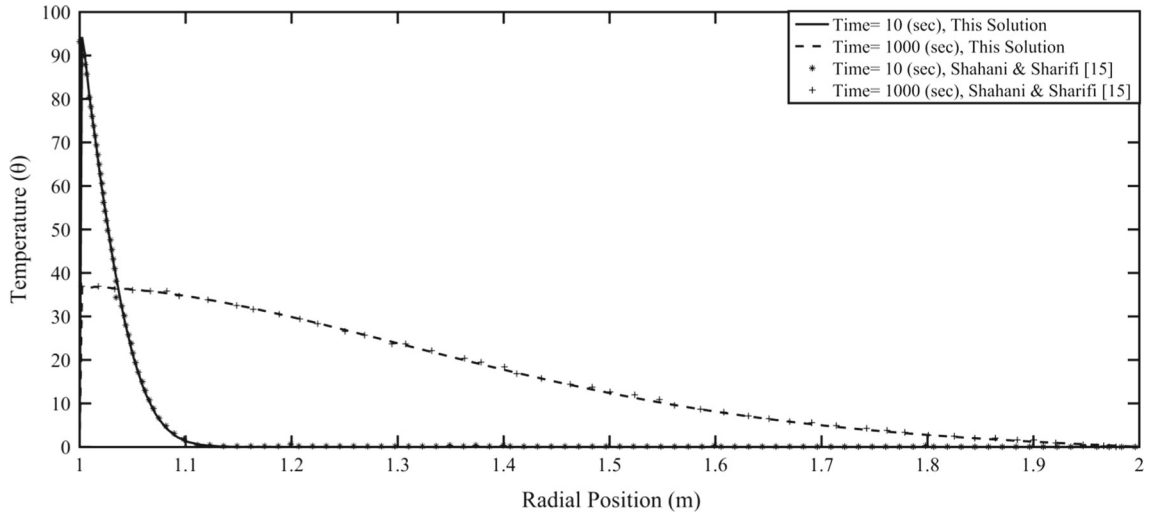

Fig. 8 Temperature distribution in isotropic cylinder

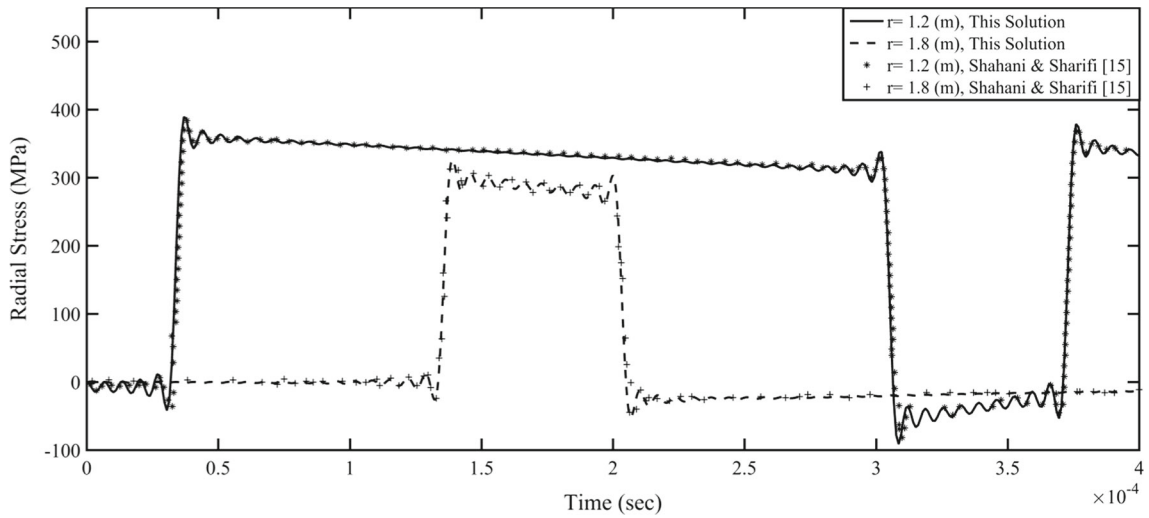

Fig. 9 History of dynamic radial stress in isotropic cylinder

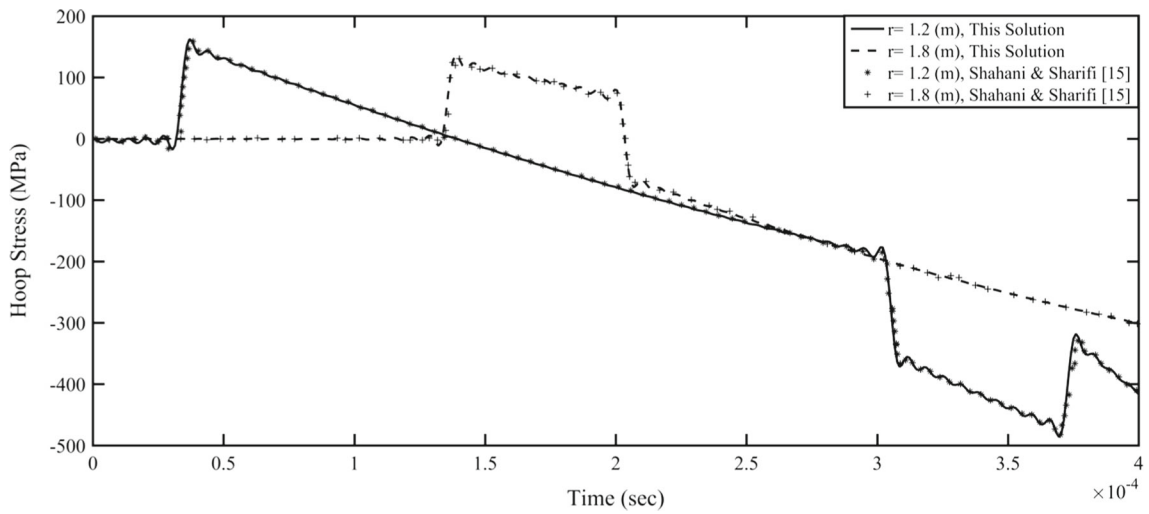

Fig. 10 History of dynamic hoop stress in isotropic cylinder

References

1. Yen, A.C., Kirmser, P.G.: On the thermal stresses in a finite circular cylinder. J. Eng. Math. **5**(1), 19–32 (1971)
2. Kardomateas, G.A.: Thermoelastic stresses in a filament-wound orthotropic composite elliptic cylinder due to a uniform temperature change. IJSS **26**(5–6), 527–537 (1990)
3. Shahani, A.R., Nabavi, S.M.: Analytical solution of the quasi-static thermoelasticity problem in a pressurized thick-walled cylinder subjected to transient thermal loading. Appl. Math. Model. **31**(9), 1807–1818 (2007)
4. Shahani, A.R., Momeni Bashusqeh, S.: Analytical solution of the thermoelasticity problem in a pressurized thick-walled sphere subjected to transient thermal loading. MMS **19**(2), 135–151 (2014)
5. Shahani, A.R., Momeni Bashusqeh, S.: Analytical solution of the coupled thermo-elasticity problem in a pressurized sphere. JThSt **36**(12), 1283–1307 (2013)
6. Yee, K.-C., Moon, T.J.: Plane thermal stress analysis of an orthotropic cylinder subjected to an arbitrary, transient asymmetric temperature distribution. J. Appl. Mech. **69**(5), 632–640 (2002)
7. Wang, X.: Thermal shock in a hollow cylinder caused by rapid arbitrary heating. J. Sound Vib. **183**(5), 899–906 (1995)
8. Cho, H., Kardomateas, G.A., Valle, C.S.: Elastodynamic solution for the thermal shock stresses in an orthotropic thick cylindrical shell. J. Appl. Mech. **65**(1), 184–193 (1998)
9. Ding, H.J., Wang, H.M., Chen, W.Q.: A solution of a non-homogeneous orthotropic cylindrical shell for axisymmetric plane strain dynamic thermoelastic problems. J. Sound Vib. **263**(4), 815–829 (2003)
10. Jabbari, M., Dehbani, H., Eslami, M.R.: An exact solution for classic coupled thermoelasticity in cylindrical coordinates. J. Press. Vessel Technol. **133**(1), 1–10 (2011)
11. Goshima, T., Miyao, K.: Transient thermal stresses in a hollow cylinder subjected to y-ray heating and convective heat losses. NuEnD **125**(2), 267–273 (1991)
12. Zhang, Q., Wang, Z.W., Tang, C.Y., Hu, D.P., Liu, P.Q., Xia, L.Z.: Analytical solution of the thermo-mechanical stresses in a multilayered composite pressure vessel considering the influence of the closed ends. Int. J. Press. Vessels Pip. **98**(1), 102–110 (2012)
13. Abd-Alla, A.M., Abd-Alla, A.N., Zeidan, N.A.: Transient thermal stresses in a transversely isotropic infinite circular cylinder. Appl. Math. Comput. **121**(1), 93–122 (2001)
14. Kouchakzadeh, M.A., Entezari, A.: Analytical solution of classic coupled thermoelasticity problem in a rotating disk. JThSt **38**(1), 1269–1291 (2015)
15. Shahani, A.R., Sharifi torki, H.: Analytical solution of the thermoelasticity problem in thick-walled cylinder subjected to transient thermal loading. MME **16**(10), 147–154 (2016). (**in Persian**)
16. Marin, M.: On weak solutions in elasticity of dipolar bodies with voids. JCoAM **82**(1–2), 291–297 (1997)
17. Marin, M.: Harmonic vibrations in thermoelasticity of microstretch materials. J. Vib. Acoust. **132**(4), 1–6 (2010)
18. Sharma, K., Marin, M.: Effect of distinct conductive and thermodynamic temperatures on the reflection of plane waves in micropolar elastic half-space. U.P.B. Sci. Bull. **75**(2), 121–132 (2013)
19. Decolon, C.: Analysis of Composite Structures. Hermes Penton Ltd, London (2002)
20. Rand, O., Rovenski, V.: Analytical Methods in Anisotropic Elasticity. Springer, Birkhauser Boston (2004)
21. Hahn, W.D., Necati O Zisik, A.: Heat Conduction, 3rd edn. Wiley, Hoboken (2012)
22. Sneddon, I.N.: The Use of Integral Transform. Mc-Graw-Hill Book Company, New York (1972)
23. Cinelli, G.: An extension of the finite hankel transform and applications. IJES **3**, 539–559 (1965)
24. Cho, H., Kardomateas, G.A.: Thermal shock stresses due to heat convection at a bounding surface in a thick orthotropic cylinderical shell. IJSS **38**, 2769–2788 (2001)